

# Evaluation of a 5-Year Cloud and Radiative Property Dataset Derived from GOES-8 Data Over the Southern Great Plains

*M. M. Khaiyer, A. D. Rapp, D. R. Doelling, and M. L. Nordeen  
Analytical Service and Materials, Inc.  
Hampton, Virginia*

*P. Minnis, W. L. Smith, Jr., and L. Nguyen  
National Aeronautics and Space Administration  
Langley Research Center  
Hampton, Virginia*

*Q.-L. Min  
Atmospheric Sciences Research Center  
State University of New York  
Albany, New York*

## Introduction

Satellite cloud analyses can provide a long-term record of microphysical, macrophysical and radiative properties over a large area. However, to have confidence in these retrievals, the results must be compared with ground truth or reliable reference sources. The layered bispectral threshold method (LBTM; Minnis et al. 1995) has been used to derive cloud and radiative properties from the eighth geostationary operational environmental satellite (GOES-8) data over a 5-year period for the Southern Great Plains (SGP) domain. These properties include cloud OD, amount, height, temperature, and thickness, total and clear-sky longwave (LW) fluxes, clear-sky temperatures, and total and clear-sky albedos. In this paper, data from several ground instruments at the SGP central facility (CF) and from the Clouds and Earth's Radiant Energy System (CERES; Wielicki et al. 1998) are used to examine the GOES-8 products.

This paper also examines the relationship between the mean skin temperature, derived from GOES-8, with the air and skin temperatures observed at the CF. The purpose of this study is to improve the estimation of clear-sky temperature used by LBTM; accurate skin temperatures are needed to establish thresholds for detecting cloudy pixels, and to better estimate the temperature underneath the clouds for retrieving cloud OD. The true clear-sky skin temperature can be derived from GOES-8 data by LBTM only when there is no cloud contamination within the scene. When a pixel is cloudy, however, it may be necessary to replace skin temperature with some function of surface air temperature. The accuracy of LBTM's cloud retrievals will be proportional to how well it estimates skin temperature; thus, the errors in skin temperature are examined for different levels of cloudiness (clear (0%), partly cloudy (1%-50%), mostly cloudy (50%-99%) and overcast (100%) cases.

## Methodology

The LBTM uses pre-designated visible (VIS; 0.63  $\mu\text{m}$ ) reflectance and infrared (IR; 11  $\mu\text{m}$ ) temperature thresholds to discriminate between clear and cloudy GOES-8 4-km pixels (Minnis et al. 1995). The GOES-8 visible radiances have been calibrated against data from the Tropical Rainfall Measuring Mission Visible Infrared Scanner (TRMM VIRS; Minnis et al. 2002a). Broadband LW (5  $\mu\text{m}$ -50  $\mu\text{m}$ ) fluxes or outgoing longwave radiation (OLR) were computed using ERBE-GOES-6 correlations of OLR and IR flux from April 1985, July 1985, and October 1986. Shortwave (SW) (0.2  $\mu\text{m}$ -0.5  $\mu\text{m}$ ) albedos were computed using a relationship based only ERBE broadband and GOES-6 SW albedos from October 1986 (Minnis and Smith 1998). The processing algorithm uses gridded synoptic sounding data to classify cloudy pixels into low (0 km-2 km), middle (2 km-6 km) and high (6 km and above) layers. Optical depths (ODs) are estimated by comparing the visible reflectances to results from a radiative transfer model parameterization. The infrared emissivity is then derived from OD to adjust cloud top temperatures. Other cloud products include cloud top heights and temperatures, and cloud amounts. The retrieval methodology is described in detail by Minnis et al (1993). The radiative parameters include the clear and total narrowband and broadband albedo, and LW fluxes.

The cloud and radiative parameters were derived on a half-hourly basis from 4-km GOES-8 data and averaged on two separate grids for the period from January 1997 through December 2001. The SGP domain covers the entire SGP and beyond (32°N-42°N; 91°W-105°W) at a 0.5° resolution. The CF domain is centered on the CF and includes nine 0.3° regions (36.16°N-37.06°N; 97.04°W-97.94°W).

For the cloud property validation, satellite-derived cloud heights and cloud fractions for the center CF grid box are compared to similar parameters derived using the active remote sensing cloud layer (ARSCL) method of Clothiaux et al. (2000), which uses the micropulse lidar (MPL) and millimeter wave cloud radar (MMCR). An indirect approach is taken to derive cloud amounts from the ARSCL best estimate of cloud base; a ratio is taken of the number of cases of cloud presence to the total data points possible within a 30-minute window. This temporally averaged cloud amount is similar to the half-hourly LBTM-derived cloud amounts. However, to smooth out discrepancies caused by the different approaches, only long-term (monthly or annual hourly) averages are compared. To evaluate LBTM-derived cloud top heights, that parameter is compared to ARSCL cloud top height data. The ARSCL cloud top heights are provided in profiles of up to ten cloud layers. The maximum cloud top heights in the profile within a half-hour window, for LBTM-defined single-level cloud cases only, are averaged and compared to the corresponding LBTM cloud top heights.

The LBTM radiative products are compared to the CERES data measured from the Terra satellite between April 2000 and February 2001. CERES broadband LW fluxes and SW albedos were averaged into 1° bins and compared to the corresponding LBTM-derived fluxes. LBTM-derived optical depths are compared to the 415 nm optical depths (half-hourly averages of 5 minute resolution retrievals) derived from multi-filter rotating shadowband radiometer (MFRSR) data over the CF (Min and Harrison, 1996).

Finally, the LBTM-computed clear-sky effective skin temperatures  $T_s$  are compared to skin temperatures  $T_{skin}$  derived from the CF Solar Infrared Radiation Station (SIRS) upwelling LW radiative fluxes, and to

air temperatures  $T_a$  from the Temperature, Humidity, Wind, and Pressure System (THWAPS). When a region is more than 20% clear, the LBTM computes a top of atmosphere (TOA) clear-sky temperature from the clear GOES-8 pixels. Otherwise, it assumes the clear-sky temperature is the surface air temperature corrected to the TOA. This is accomplished by using a simple radiative transfer model employing the correlated  $k$ -distribution coefficients appropriate for the GOES-8 IR channel (Minnis et al. 2002b). To compare the derived parameter to SIRS and THWAPS, the LBTM-defined clear-sky IR temperature  $T_{cs}$  is converted to  $T_s$  by removing the atmospheric effects and accounting for the surface emissivity, which is taken from Smith et al. (1999).  $T_{skin}$  is derived from the SIRS data by using the Stefan-Boltzmann equation assuming the LW surface emissivity is equal to the IR surface emissivity. The IR surface emissivity for the CF area ranged from 0.970 to 0.985 during the year.

## Results

Figures 1 and 2 show examples of the large domain daytime only ( $SZA < 80^\circ$ ) 5-year means (1997-2001) for some of the LBTM-derived parameters. The average clear-sky SW albedo (Figure 1a) derived from the VIS clear-sky reflectances is 13.6% with a standard deviation ( $\sigma$ ) of 2.0%. The maximum yearly mean for this parameter occurred in 2001 (14.0%) with a minimum of 13.3% in 1999. The albedo generally increases from east to west with decreasing vegetation. The average domain total cloud amount is 50.6% with a regional  $\sigma$  of 7.7% (Figure 1b) increasing from less than 40% in the southwest to more than 60% in the northeast part of the domain. Yearly domain averages for total cloud amount varied from a minimum of 48.2% in 1999 to a maximum of 53.4% in 1997.

The 5-year mean total cloud VIS optical depth (Figure 1c) is 17.0 with  $\sigma = 1.7$ . It increases mainly from west to east with a maximum in the northeast corner. The minimum annual mean OD was 15.9 in 1999 compared to 2001 maximum of 17.9. Total cloud center height (Figure 1d) averaged 4.9 km, with a  $\sigma = 0.4$  km. The annual means for this parameter ranged from 4.7 km in 1998 to 5.1 km in 1997. Mean clouds are highest over the Rockies, along the western boundary of the domain. The mean annual total broadband SW albedo (Figure 2b) is 30.0% with a  $\sigma = 2.1\%$ . The albedo increases from less than 30% in the southwest to 35% in the northeastern corner. The domain average reached a minimum of 29.2% in 1999 and a maximum in 1997 of 30.6% in concert with the cloud amounts. The mean OLR (Figure 2a) was  $241.1 \text{ Wm}^{-2}$  with a standard deviation of  $8.2 \text{ Wm}^{-2}$ . Mean OLR was at a maximum in 1999 and a minimum in 1997 ( $244.5$  versus  $236.6 \text{ Wm}^{-2}$ ). High cloud (above 6 km) amounts (Figure 2c) averaged 22.4% with  $\sigma = 3.5\%$ . They were most common in the eastern half as well as the northwest corner of the domain. The maximum high cloud amount average (23.7%) occurred in 1997, with a minimum of 20.4% in 1998. The highest clouds occurred in the southwest and southeast corners of the domain. The mean high-cloud center height (Figure 2d) is 9.3 km with  $\sigma = 0.4$  km; this parameter showed very little variation, ranging between 9.2 km - 9.3 km for all 5 years.

Seasonal means of the parameters shown in Figures 1 and 2 were also computed. Winter is defined as January-March, spring as April-June, summer as July-September, and autumn as October-December. The maximum total and high cloud center heights and OLR were in summer, with values of 5.4 km ( $\sigma = 0.6\text{km}$ ), 10.5 km ( $\sigma = 0.7\text{km}$ ) and  $268.7 \text{ Wm}^{-2}$  ( $\sigma = 8.3 \text{ Wm}^{-2}$ ), respectively. The corresponding

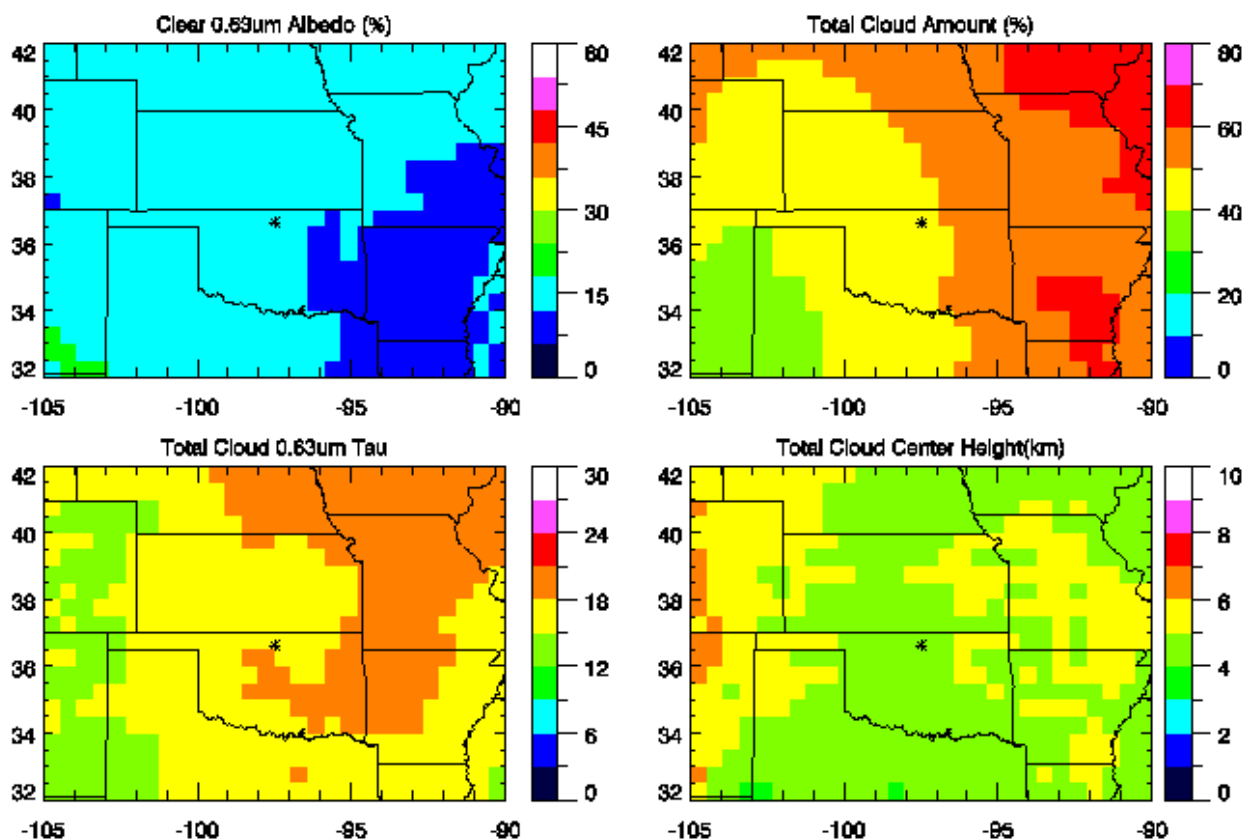


**Figure 1.** Clockwise from top left: Daytime-only 5 year (1997-2001) averages of clear-sky visible albedo, total cloud amount, total cloud visible OD, and total cloud center height.

minima in autumn for total cloud center height was 4.5 km ( $\sigma = 0.4\text{km}$ ). The high cloud center height and OLR were minimum in winter, at 8.1 km (0.3km) and was  $219 \text{ Wm}^{-2}$  ( $\sigma = 9.5 \text{ Wm}^{-2}$ ), respectively. Winter also had the maximum cloud amount (58.8%,  $\sigma = 8.1\%$ ), and total and clear-sky SW albedos 37.2% ( $\sigma = 3.6\%$ ) and 15.4% ( $\sigma = 2.7\%$ ), respectively. The corresponding minima for these parameters were found in summer, with 44.1% ( $\sigma = 9.3\%$ ), 25.0% ( $\sigma = 1.5\%$ ), and 12.8% ( $\sigma = 1.9\%$ ), respectively. Spring had a maximum of high cloud amount (24.8%,  $\sigma = 3.6\%$ ), with a minimum in autumn (18.9%,  $\sigma = 1.9\%$ ). Optical depth was highest in autumn (21.9,  $\sigma = 2.8$ ) and lowest in summer (11.5,  $\sigma = 1.9$ ).

Similar statistics are available for all of the parameters derived with the LBTM. Mean diurnal variations of many parameters can also be computed for any time scale. Even though the results are presented here for daytime only, the results are available for nighttime hours. Cloud heights are less certain at night because height corrections for semi-transparent clouds require estimates of cloud OD. Because cloud layer amounts depend on the actual heights, their values are also less certain at night. Nevertheless, the results should be useful for studying the daytime variations of all parameters and for examining the diurnal cycles of total cloud amounts.

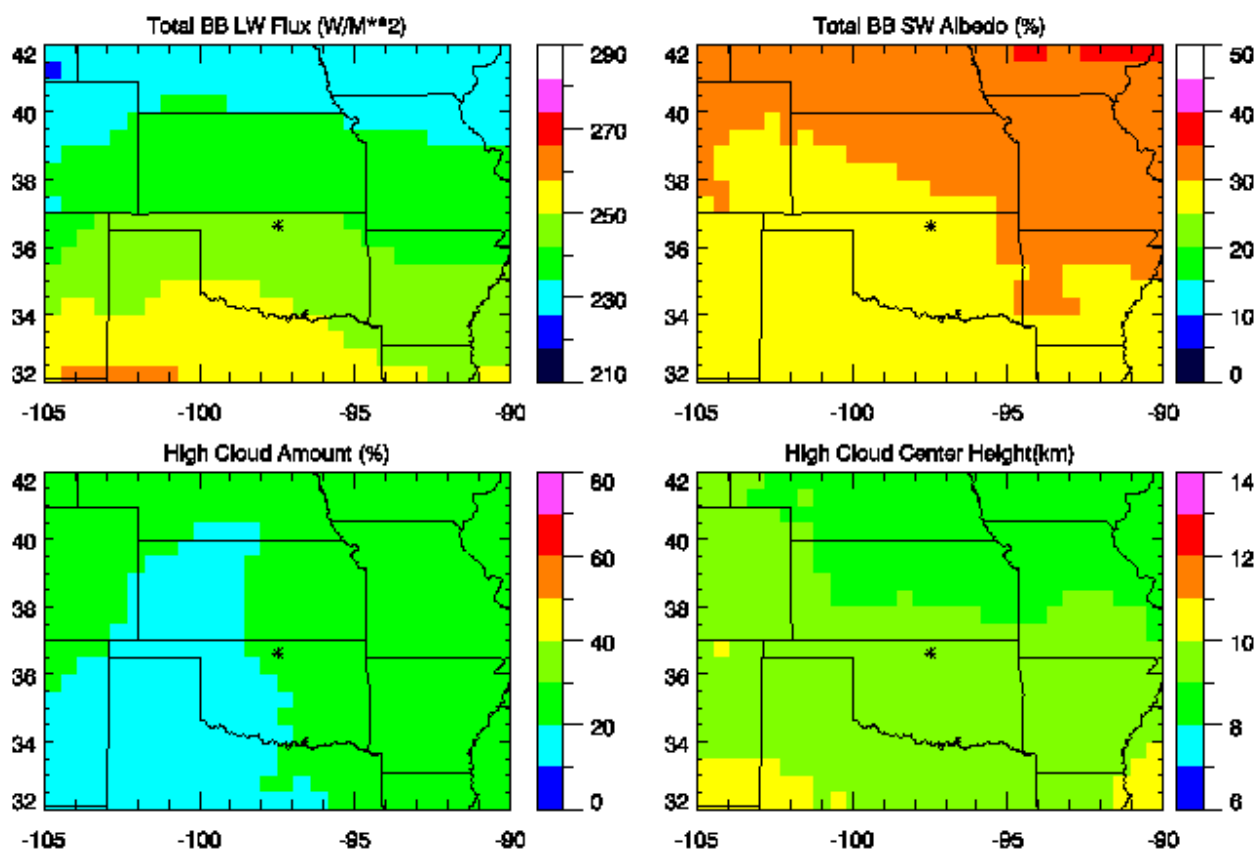


**Figure 2.** Clockwise from top left: Daytime-only 5 year (1997-2001) averages of total broadband LW flux, total broadband SW albedo, high cloud amount, and high cloud center height.

## Discussion

The cloud amounts in Figure 1b are generally consistent with the 11-year mean total cloud amounts derived from surface observations between 1971 and 1981. The  $5^\circ$  gridded means from Warren et al. (1986) for the domain between  $30^\circ\text{N}$  and  $45^\circ\text{N}$ ,  $90^\circ\text{W}$  to  $105^\circ\text{W}$  yield an annual average of 51.9%, a value that is 1.3% greater than observed here. The 11-year cloud amounts vary from 43% in the southwestern corner to 60% in the northeastern corner with a secondary maximum in the southeastern corner as in Figure 1b. The LBTM results are presented here for daytime only; when nighttime values are considered, the LBTM cloud amount average is significantly smaller than the surface-observed values. This highlights the need for improved nocturnal retrievals within LBTM.

This discrepancy between daytime and nighttime LBTM retrievals can also be seen when comparing to ARSCL cloud amounts. Figure 3 shows comparisons of mean cloud amount and height from the ARSCL and LBTM results over the CF. Time series of monthly-averaged daytime-only cloud amounts from ARSCL MPL-MMCR cloud base best estimate versus LBTM from 1997-2001 follow a similar trend in most cases (Figure 3a). Figure 3b shows a scatterplot of the monthly-averaged cloud amounts shown in (a). RMS differences are 12.9% for the period when all data is considered, and 12.0% when daytime-only data is compared; corresponding average differences (ARSCL-LBTM) are 5.3% for all

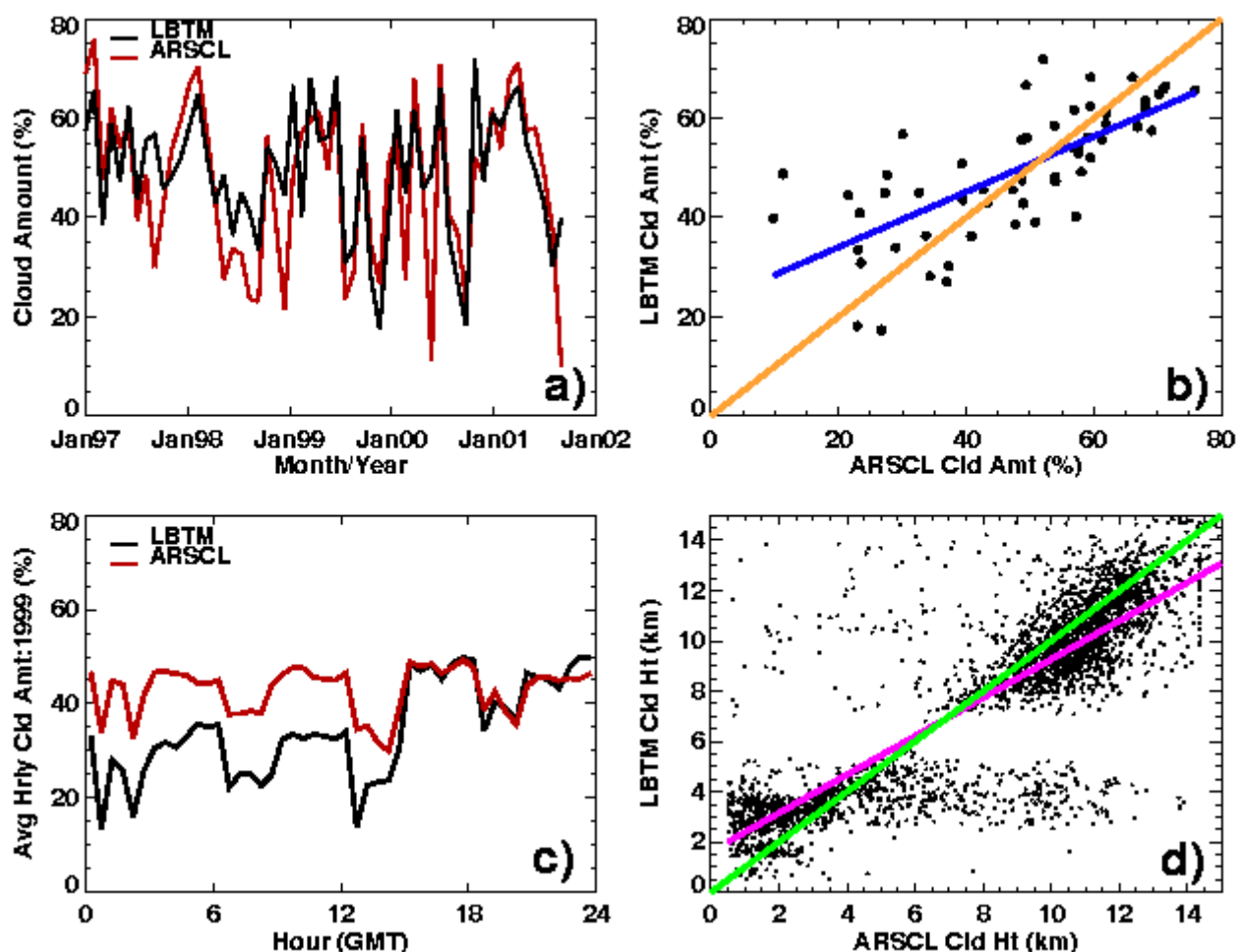


**Figure 3.** Comparisons of LBTM-derived and ARSCL-derived cloud parameters: a) 1997-2001 daytime-only monthly-averaged cloud amounts (ARSCL red, LBTM black), b) scatterplot of LBTM and ARSCL monthly-averaged cloud amounts from 1997-2001, c) LBTM (black) and ARSCL (red) hourly-averaged cloud amounts for the year 1999, and d) scatterplot comparison of LBTM and ARSCL cloud top heights for single layer clouds in 1997-2001.

data, and -2.4% for daytime data only. Hourly-averaged cloud amounts derived from the ARSCL for the year 1999 are compared to LBTM-derived amounts (Figure 3c). LBTM values are usually lower than ARSCL during the night, but the two quantities are very comparable during the day; the cloud amount trend can be seen throughout all times.

LBTM retrieves cloud top height directly and depends on the use of a sounding to convert temperature to height. A comparison of the 1997-2001 cloud top heights derived from ARSCL compared to LBTM-derived cloud top heights is shown in Figure 3d. Only data for  $SZA < 70^\circ$ , cloud heights above 0.5 km, and single-layered clouds as determined from LBTM, were used. The values for low cloud and high cloud show significant correlation along the one-to-one line, but there are many outliers. The two classes of outliers are LBTM significantly underpredicting ARSCL-derived high cloud top heights, and LBTM predicting higher cloud top heights than those of ARSCL. These differences are likely due to a

number of factors. Half-hour temporal cloud top height averages, as calculated here with ARSCL data, may not reflect the areal average within a  $0.3^\circ$  box produced by LBTM. This would introduce a more random error (depending on wind speed and direction, for example), causing both under- and over-predictions of cloud-top height. In terms of systematic errors, LBTM can only derive clouds in three possible height categories, whereas ARSCL can detect up to ten layers. Also, LBTM can only detect one radiating center of cloud layer in any given location, and cannot derive a cloud layer profile as ARSCL can. Thus, the LBTM underestimates are likely cases of optically thin clouds overlaying thicker, warmer mid-level or low clouds and are interpreted as single-layer clouds. Conversely, when LBTM-derived cloud-top heights are higher than those from ARSCL, it may be because the ARSCL ground-based instruments are looking up through optically thick clouds, and thus may not detect the cloud tops, especially if the particle sizes are small. Many of the cases where LBTM predicts higher cloud top heights than ARSCL can be attributed to this. Other cases, especially those for low clouds, may be due to the lack of sufficient vertical resolution in the soundings, so that clouds under inversions are mistakenly assigned altitudes above the inversions. In general, the data are well-correlated ( $R^2 = 0.71$ ), but due to the aforementioned outliers, the RMS error is 2.3 km for all data.

The 11-year averages of 3-hourly data from Warren et al. (1986) yield a mean diurnal range in total cloud fraction of  $\sim 15\%$  with a mean time of maximum cloudiness around local noon. The diurnal variations in 3-hourly averages from the satellite indicate a larger diurnal range of 18.9% with a maximum of 51.9% near local noon. The LBTM results are consistent with the long-term observer data but may overestimate the magnitude of the diurnal range. An underestimate of low clouds at night, an artifact of using an IR channel alone, could explain the  $\sim 4\%$  greater satellite-based diurnal range, and the ARSCL-LBTM differences.

Figure 4a shows the comparison of LBTM-derived optical depth retrievals for the CF grid box to MFRSR-derived values. MFRSR values are included for five minute periods where the direct beam is completely extinguished. When there are at least six contiguous 5 minute retrievals, the values are binned and averaged to compare to the LBTM half-hourly retrievals. Cases of LBTM-defined single layer low cloud (100% cloud between 0-2 km height), for  $SZA < 80^\circ$ , are included. RMS difference between LBTM and MFRSR-derived OD is 19.2 when all cases are taken into account, and 14.7 when ODs 1 - 80 are considered. Figure 4b shows the VISST (Visible Infrared Solar Split-Window Technique)  $0.3^\circ$ -averaged pixel-level retrievals compared to LBTM CF  $0.3^\circ$  grid box and MFRSR-derived values, for cases throughout 2000. The comparison again includes 100% cloud only, but for  $SZA < 70^\circ$ . The data fall close to the one-to-one line for  $OD < 80$ . RMS errors for  $OD < 80$  are 6.9 (MFRSR-LBTM) and 6.1 (MFRSR-VISST); for all OD they jump to 18.0 (MFRSR-LBTM) and 16.9 (MFRSR-VISST). Figure 4c shows a comparison of surface and aircraft-derived optical depths against GOES-8 (VISST) derived OD during March 2000 (Dong et al. 2002). Since VISST and LBTM OD agree fairly well (rms error = 6.2 for cases shown in Figure 2b for 2000), it is assumed LBTM OD retrievals agree with the radar-derived values.

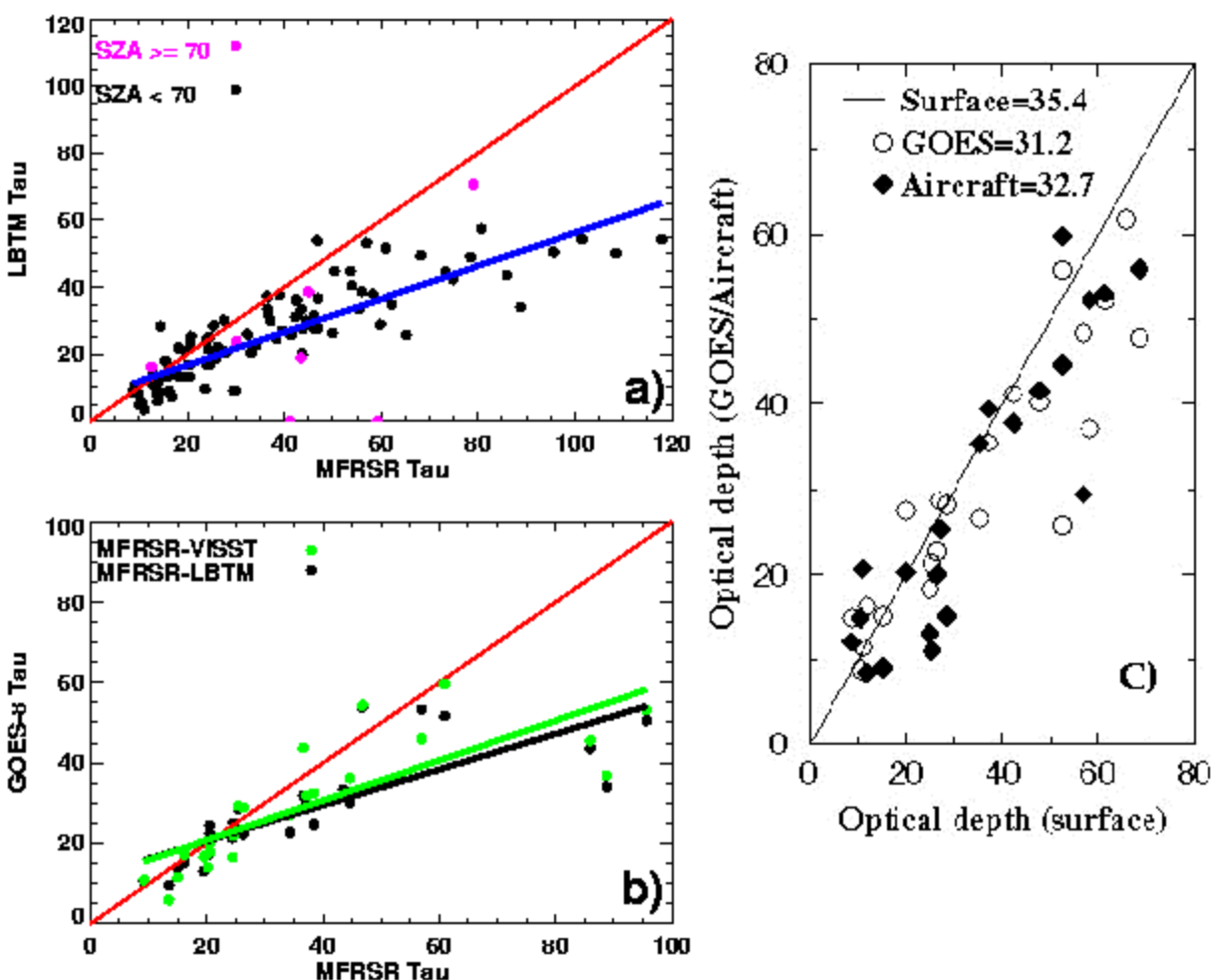


**Figure 4.** a) Comparison of 1997-2000 LBTM-derived and MFRSR-derived ODs for single layer warm clouds, b) comparison of year 2000 LBTM-derived, VISST-derived, and MFRSR-derived ODs, and c) comparison of surface-based radiometer- and radar-derived OD and aircraft-derived values for March 2000 Cloud IOP (Dong et al. 2002).

Figure 5a shows the broadband SW flux CERES-GOES comparison for April 2000. There is better agreement between CERES and GOES for SW than for LW quantities. The mean bias (CERES average albedo - GOES average albedo) is  $-0.004$  and the rms error is  $0.017$ . The comparison for February 2001 is shown in Figure 5b. The bias is  $0.086$  and the rms error is  $0.047$ . The disagreement between the albedos is likely due to snow, which was not included in the original narrowband-broadband relationship. The LW flux CERES-GOES comparison for April 2000 shows more scatter than the SW comparisons. The bias is  $-7.5 \text{ Wm}^{-2}$  (CERES OLR - GOES8 OLR) and the rms error is  $13.8 \text{ Wm}^{-2}$ . The comparison for February 2001, with bias  $-6.3 \text{ Wm}^{-2}$  and rms error  $10.9 \text{ Wm}^{-2}$ , is shown in Figure 5d.



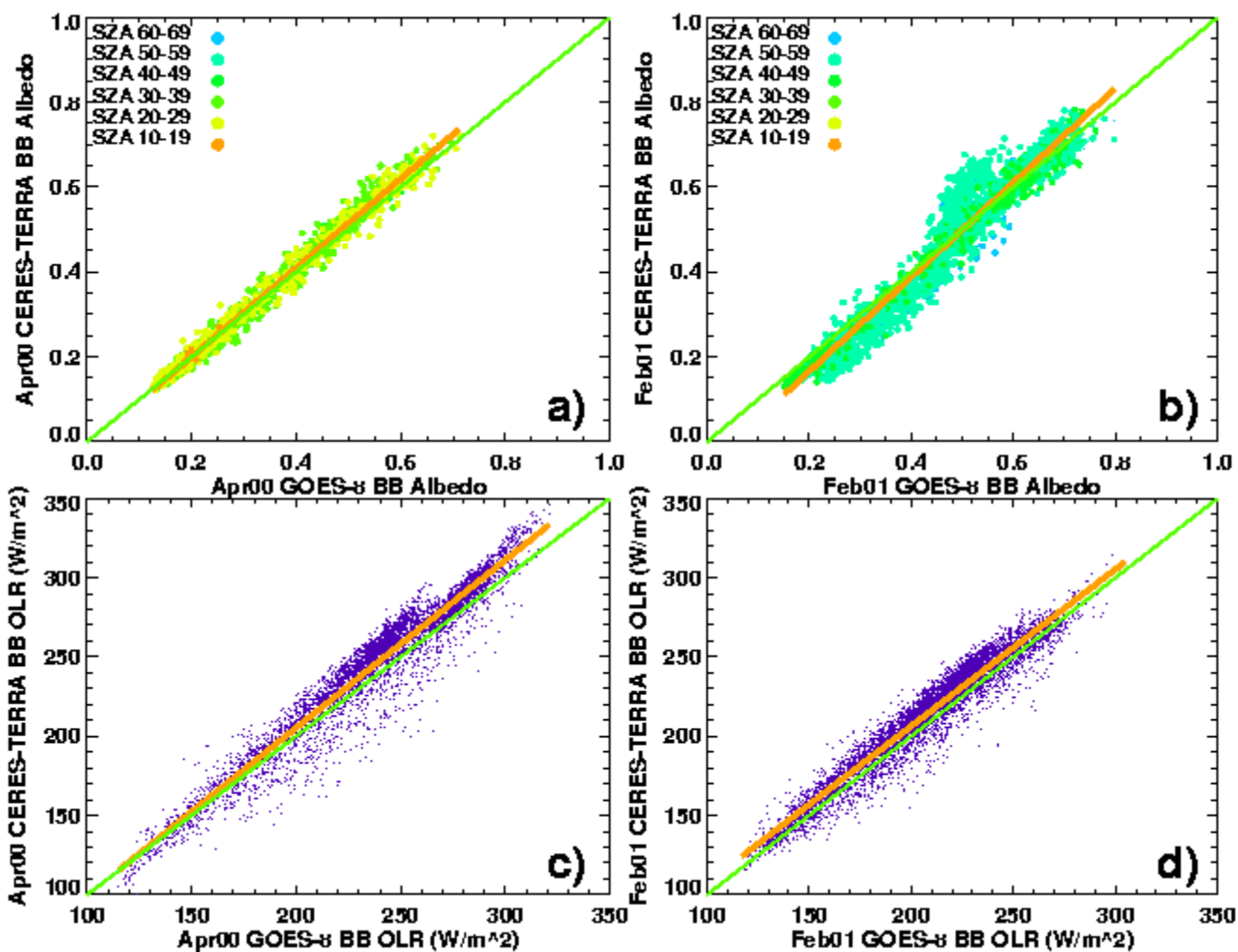


**Figure 5.** CERES-TERRA and GOES8 broadband SW flux comparisons for a) April 2000; b) February 2001; and CERES-TERRA and GOES8 broadband LW flux comparisons for c) April 2000; and d) February 2001.

Five-minute averages of 1998 SIRS-derived skin temperature, five minute resolution THWAPS air temperature, and 30-minute resolution LBTM-computed clear-sky effective skin temperature (CST) scatterplots are shown in Figure 6. Figure 6a shows skin temperature against air temperature and Figure 6b shows the CST for clear cases. Figures 6c and d show the same relationships, for 100% cloudy cases. Limits of temperatures 260 K to 320 K for all temperature values have been imposed. All correlations are high ( $R^2$  ranges from 0.91 - 0.96), but the scatter is least for the cloudy case of skin against air temperature. Figure 7 shows skin temperature, air temperature, and LBTM-derived CST diurnal plots for clear days in January 1998 (a) and April 1998 (b). The temporal lag in air temperature compared to skin temperature is greatest in April 1998 when the insolation is higher. CST closely follows the actual skin temperature. Figure 8 shows diurnal plots of hourly-binned January 1998 absolute (a) and RMS differences (c) in skin temperature versus air temperature, and skin temperature versus CST in (b) and (d), respectively. The overcast (100% cloud) cases show the lowest absolute and rms errors for skin temperature against air temperature; all cloud classifications show higher errors

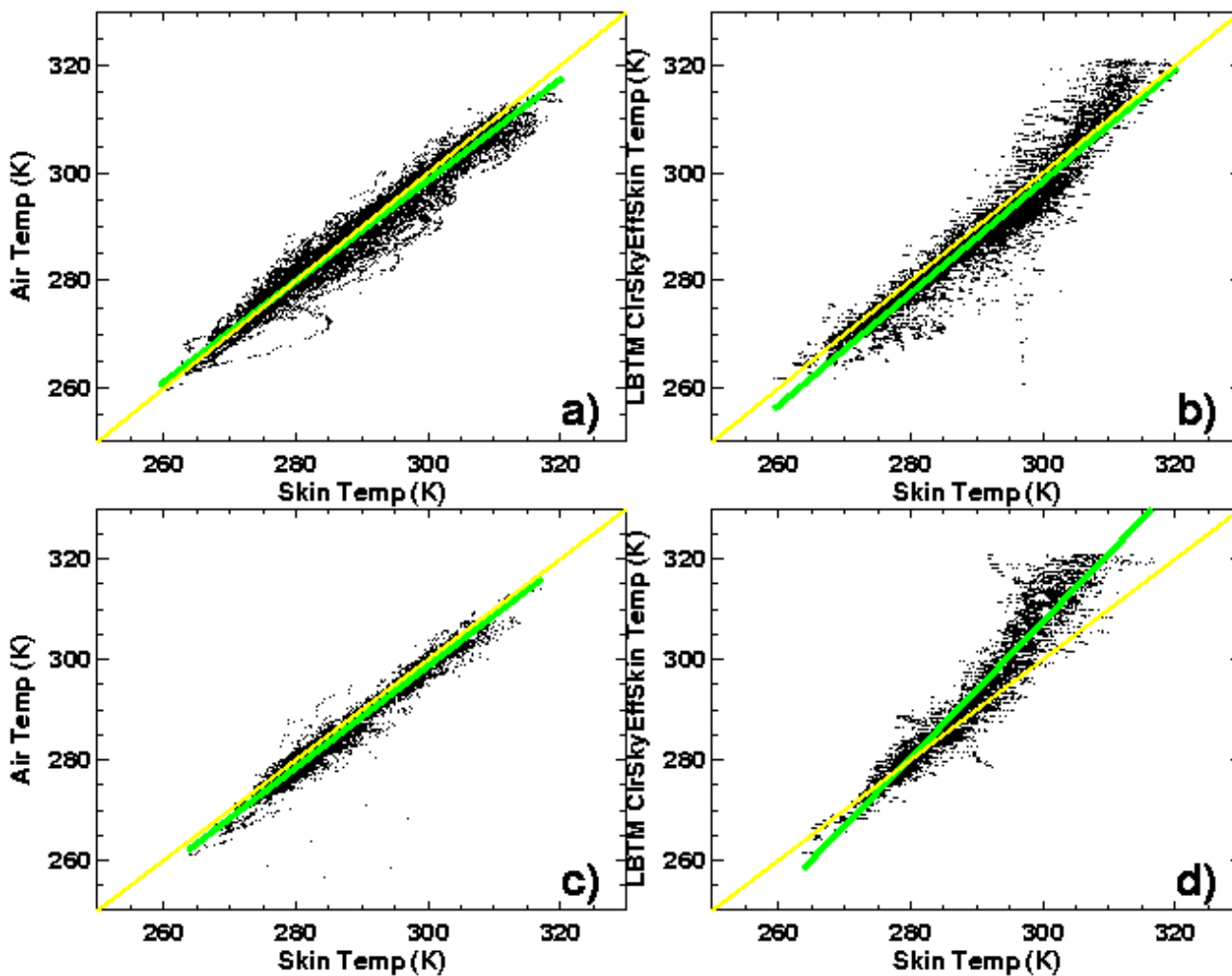


**Figure 6.** a) 1998 temperature comparisons for clear-sky a) THWAPS air temperature compared to 5 minute-averaged SIRS-derived skin temperature, b) LBTM-computed CST compared to SIRS-derived skin temperature, c) same as a) for 100% cloud cover, and d) same as b) for 100% cloud cover.

during the day than at night. Comparisons of skin temperature and CST show again that the lowest errors are usually for the overcast case. Nighttime errors are worse than daytime for all cases, and of these, mostly and partly cloudy data errors are highest. This illustrates the differences in surface-based and GOES-derived skin temperatures at night. SIRS skin temperatures will fluctuate proportionally to the actual cloud cover overhead, whereas LBTM (GOES8)-defined skin temperature will be biased by the colder cloud-free data; it cannot measure the surface warmed by the nighttime cloud cover that SIRS can.

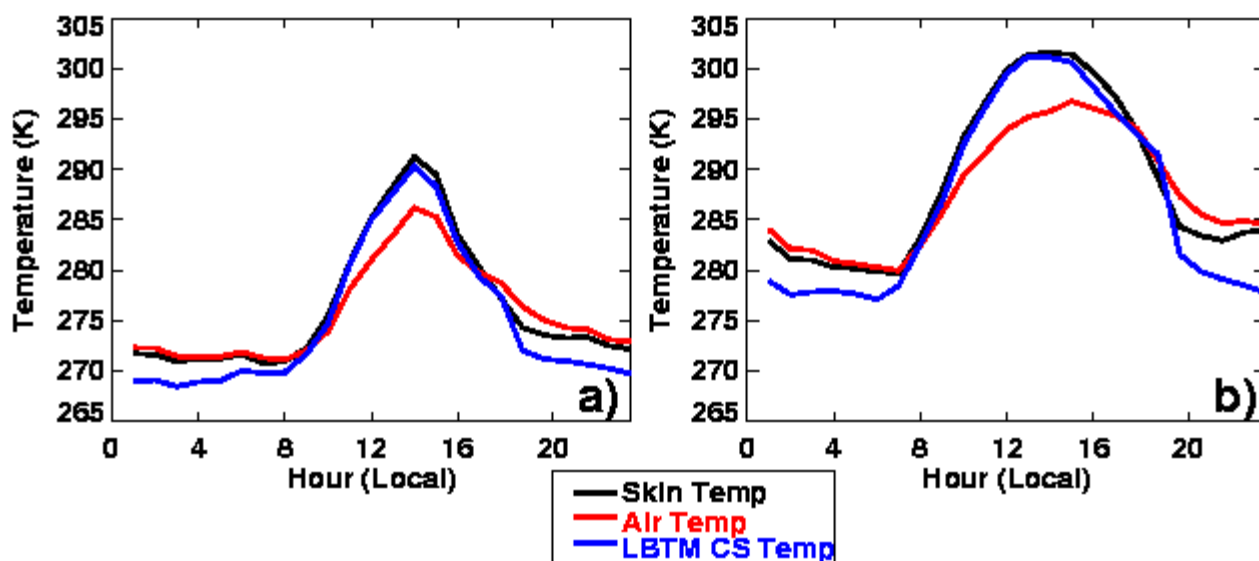


**Figure 7.** Comparison of SIRS-derived skin temperature (black), THWAPS air temperature (red), and LBTM-computed CST (blue) for clear days in a) January 1998, and b) April 1998.

## Conclusions and Future Work

Five year averages of LBTM-derived parameters were presented. The daytime-only LBTM averaged total cloud amount results agree well with day and night surface-based observations (Warren et al, 1986), however, when nighttime cloud retrievals are added in to the LBTM averages, the LBTM amounts are smaller than the surface values on average. Autumn and winter maxima in OD, total cloud amount, and clear-sky and total broadband SW albedos are consistent with more frequent synoptic-scale storms and lower solar zenith angles (greater albedos). The occurrence of snow during the winter may also cause some bias in cloud optical depth or part of the domain. These results, while providing some useful long-term climatological information, indicate the need for better nighttime retrieval, as well as retrievals of cloud over snow.

Optical depth validation shows LBTM agrees fairly well with MFRSR-derived values in low optical depth cases ( $OD < 30$ ), where the rms differences are 6.7 for 1997-2000 LBTM-MFRSR. Agreement decreases when all optical depths are considered. LBTM and VISST both showed good agreement for the 2000 OD cases compared to MFRSR for  $OD < 80$ . Rms errors for both GOES-8 derived datasets were  $\sim 6-7$  for  $OD < 80$ , while the RMS difference doubled when all cases of OD were considered. However, VISST-derived values (which agree with LBTM) agreed well with aircraft and surface-derived OD (Dong et al. 2000) for March 2000 case. More investigation into the cause of these optical depth differences is needed.

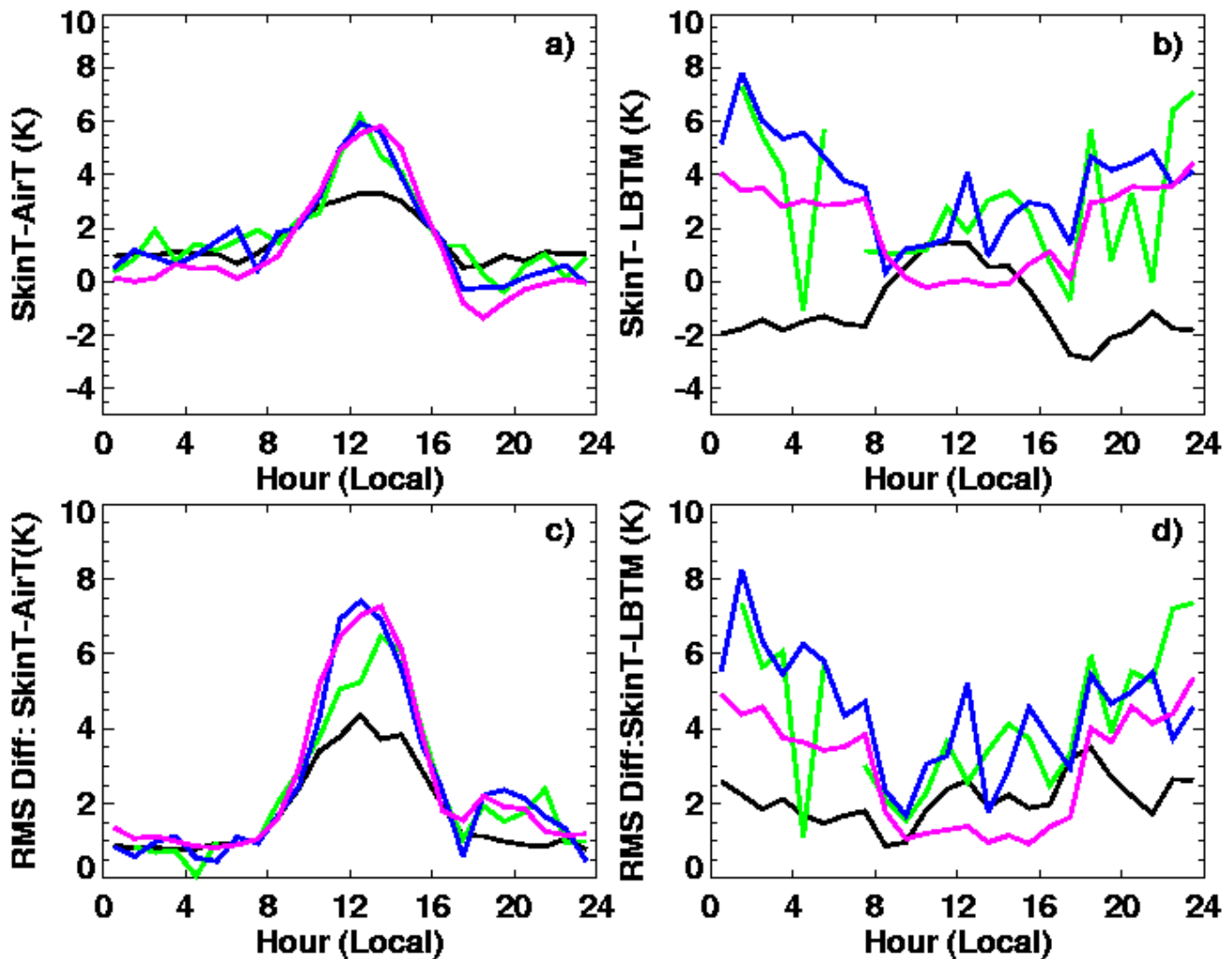


**Figure 8.** Diurnal plots of hourly-binned January 1998 absolute differences in skin temperature and a) air temperature, b) LBTM-computed clear-sky temperature, and RMS differences in skin temperature, c) air temperature, and d) LBTM-computed clear-sky temperature. Black lines denote overcast conditions (100% cloud cover), green denotes mostly cloudy (50-99% cloud cover) blue represents partly cloudy (1-50% cloud cover), and pink denotes clear (0% cloud cover).

Monthly cloud amount comparisons from 1997-2001 between LBTM and ARSCL showed a similar trend, and were best when only daytime data was considered. LBTM significantly underpredicts at night compared to the ARSCL. The rms difference for 1997-2001 daytime only cases was 12.0%, and was 12.9% when all cases were considered. Half-hourly averaged cloud-top heights between LBTM and ARSCL showed a significant correlation ( $R^2 = 0.71$ ) but also had a number of outliers, due to the differences in the nature of the cloud classification methods. Due to these outliers, the RMS difference in cloud top heights for 1997-2001 was fairly high at 2.3 km.

Broadband CERES GOES-8 LW flux comparisons agreed better for low OLR for the period April 2000 through February 2001, but the biases ranged from  $-9.2 \text{ Wm}^{-2}$  in May 2000 to  $2.4 \text{ Wm}^{-2}$  in Aug00. For the period, the average bias was  $-4.2 \text{ Wm}^{-2}$ , with rms errors ranging from  $10.1 \text{ Wm}^{-2}$  in December 2000

to  $15.9 \text{ Wm}^{-2}$  in May 2000. Shortwave flux comparisons were somewhat better except for winter months with snow contamination. The bias ranges from -0.001% in June 2000 to 0.009 in February 2001. The average bias error is 0.006 with an rms error ranging from 0.013 in August 2000 to 0.047 in February 2001. New conversion functions that will be developed using CERES data should improve the GOES-8 fluxes.

Comparisons of LBTM-derived clear-sky effective skin temperature with SIRS skin temperature and THWAPS surface air temperature indicate that the most consistently low errors are usually for overcast and clear cases. Partly and mostly cloudy cases, especially at night, provide a challenge for LBTM in defining accurate clear-sky temperature. Unlike SIRS, GOES-8 cannot measure the nighttime surface warmed by clouds; it can only see to the surface in the colder cloud-free areas. Overall the comparisons indicate that the LBTM-defined values are fairly accurate. More work is needed to determine the relationships among the various temperatures during varying cloud cover conditions. These error analyses will help in improving skin temperature estimation, clear-sky thresholds, cloud-detection thresholds, and surface emitted LW flux.

## Acknowledgment

The ARSCL, SIRS, THWAPS, and GOES-8 data were obtained from the Atmospheric Radiation Measurement (ARM) Program sponsored by the U.S. Department of Energy, Office of Science, Office of Biological and Environmental Research, Environmental Sciences Division. Periods of GOES-8 data, as well as surface and sounding data used in the retrievals, were obtained from the Space Science and Engineering Center at University of Wisconsin-Madison. The CERES-Terra data was obtained from the NASA Langley Research Center Atmospheric Sciences Data Center. This research was sponsored by ITF No. 214216-A-Q1 from Pacific Northwest National Laboratory.

## References

- Clothiaux, E. E., T. P. Ackerman, G. G. Mace, K. P. Moran, R. T. Marchand, M. Miller, and B. E. Martner, 2000: Objective determination of cloud heights and radar reflectivities using a combination of active remote sensors at the ARM CART sites. *J. Appl. Meteorol.*, **39**, 645-665.
- Dong, X., P. Minnis, G. G. Mace, W. L. Smith, Jr., M. Poellot, and R. Marchand, 2002: Comparison of stratus cloud properties deduced from surface, GOES, and aircraft data during the March 2000 ARM Cloud IOP. *J. Atmos. Sci.*, accepted.
- Min, Q.-L., and L. Harrison, 1996: Cloud Properties derived from surface MFRSR measurements and comparison with GOES results at the ARM SGP site. *Geophys. Res. Lett.*, **23**, 1641-1644.
- Minnis, P., P. W. Heck, and D. F. Young, 1993: Inference of cirrus cloud properties using satellite-observed visible and infrared radiances, Part II: Verification of theoretical cirrus radiative properties. *J. Atmos. Sci.*, **50**, 1305-1322.

- Minnis, P., L. Nguyen, D. F. Young, D. R. Doelling, D. P. Kratz, and W. F. Miller, 2002a: Rapid calibration of operational and research meteorological satellite imagers, Part I: Use of research satellite visible channels as references. *J. Atmos. Oceanic Technol.*, in press.
- Minnis, P., L. Nguyen, D. F. Young, D. R. Doelling, D. P. Kratz, and W. F. Miller, 2002b: Rapid calibration of operational and research meteorological satellite imagers, Part II: Comparison of infrared channels. *J. Atmos. Oceanic Technol.*, in press.
- Minnis, P., and W. L. Smith, Jr., 1998: Cloud and radiative fields derived from GOES-8 during SUCCESS and the ARM-UAV Spring 1996 Flight Series. *Geophys. Res. Ltrs.*, **25**, 1113-1116.
- Minnis P., W. L. Smith, Jr., D. P. Garber, J. K. Ayers, and D. R. Doelling, 1995: Cloud properties derived from GOES-7 for Spring 1984 ARM intensive observing period using Version 1.0.0 of ARM satellite data analysis program. NASA RP 1366, p. 58.
- Smith, W. L., Jr., P. Minnis, D. F. Young, and Y. Chen, 1999: Satellite-derived surface emissivity for ARM and CERES. *Proc. AMS 10<sup>th</sup> Conf. Atmos. Rad.*, June 28 - July 2, 410-413, Madison, Wisconsin.
- Warren, S. G., C. J. Hahn, J. London, R. M. Chervin, and R. L. Jenne, 1986: Global distribution of total cloud cover and cloud types amounts over land. NCAR Technical Note *NCAR/TN-273+STR*, p. 224.
- Wielicki, B. A., B. R. Barkstrom, B. A. Baum, T. P. Charlock, R. N. Green, D. P. Kratz, R. B. Lee, P. Minnis, G. L. Smith, D. F. Young, R. D. Cess, J. A. Coakley, Jr., D. A. H. Crommelynck, L. Donner, R. Kandel, M. D. King, A. J. Miller, V. Ramanathan, D. A. Randall, L. L. Stowe, and R. M. Welch, 1998: Clouds and the earth's radiant energy system (CERES): Algorithm overview. *IEEE Trans. Geosci. Remote Sens.*, **36**, 1127-1141.